Fundamental and Practical Studies of Metal Contacts on Mercury Zinc Telluride

Sponsored by

The Defense Advanced Research Projects Agency (DoD)

Administered through

The Office of Naval Research

ARPA Order: 5674 FRC H414 dated 01/86 August 22

Contract No. N00014-86-K-0854

Final Technical Report: September 1, 1986 to August 31, 1989

Principal Investigator: W. E. Spicer
Stanford Electronics Laboratories
Stanford University
Stanford, CA 94305-4055
(415) 723-4643

Final Technical Report
DARPA Contract No. N00014-86-K-0854
September 1, 1986 - August 31, 1989

A. K. Wahi, I. Lindau, and W. E. Spicer
Stanford Electronics Laboratories, Stanford University, Stanford, CA 94305

Section I - Introduction

How the metal overlayer grows and chemically interacts with the substrate in metal/II-VI systems such as CdTe and ZnTe has practical importance for the electrical characteristics of metal contacts to these materials. Additionally, by studying metal interfaces with these binaries, we gain insight into the role of the weak Hg-bonding in the alloys HgCdTe and HgZnTe during metal contact formation, where severe Hg depletion on the order of 20-60% from the top few layers of the HgCdTe substrate is typically observed upon metal deposition. We report here in detail results of our comparative study of the interfacial chemistry and band bending behavior for Al, In, Ag, and Pt overlayers on vacuum-cleaved *p*-CdTe and *p*-ZnTe (110) using both UPS and XPS. A range of metal-substrate reactivities have been considered: Al reacts strongly with Te, Ag moderately, and In minimally, with no evidence seen for In reaction on ZnTe. Pt exhibits strong alloying behavior with both Cd and Zn. We compare these results for the binaries to metal/HgCdTe interface formation. We find that Hg loss can significantly influence the extent of reaction and/or intermixing for these overlayers, with resulting disruption either inhibiting or facilitating chemical interaction. These results are discussed in Section II.

We further consider band bending at these metal/CdTe and metal/ZnTe interfaces, with the objective of correlating Fermi level movement in the bandgap during metal deposition with interfacial chemistry and morphology of the overlayer. All four metals are found to yield Schottky barriers on CdTe and ZnTe, with a narrow range of final Fermi level positions, $E_{fi} = E_f - E_{VBM}$, observed on CdTe, from 0.9 to 1.05 ± 0.1 eV, and on ZnTe from 0.65 to 1.0 ± 0.1 eV. The prediction of the metal-induced gap states (MIGS) model that a difference in barrier height exists for two semiconductors dependent upon their band lineup (valence band offset) is examined and

found to agree with experiment for Ag, Pt and Al, but not for In. For the highly reactive Al, no evidence for the overlayer metallicity required for MIGS to operate is seen on CdTe or ZnTe until after band bending has stabilized. Reaction and intermixing for Al, Ag, and Pt overlayers on CdTe and ZnTe indicate these interfaces are not ideal. The possible role of defects at these four metal/CdTe and metal/ZnTe interfaces provides a consistent explanation for the final Fermi level positions observed.

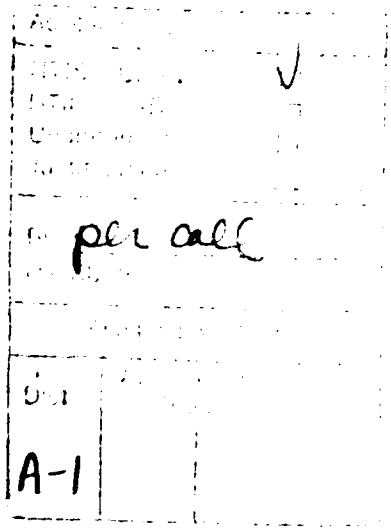

Section II - Interfacial Chemistry and Band Bending of Metals on CdTe and ZnTe (110)

I. INTRODUCTION

Although much work is reported in the literature on the electrical properties (barrier height or ohmic nature) of a wide range of metal contacts to CdTe[1,2], relatively few studies are available examining CdTe metal interface formation in detail.[3] We have investigated interfacial chemistry and morphology in conjunction with band bending behavior using photoemission for the metals In, Al, Ag, and Pt on CdTe (E_g = 1.5 eV) and the wider bandgap ZnTe (E_g = 2.2 eV). How the metal overlayer grows and chemically interacts with the substrate in these II-VI systems has practical importance for the electrical characteristics of metal contacts to these materials. These comparative studies are also important in relation to metal/HgCdTe and metal/HgZnTe interface formation, where HgZnTe has been proposed as structurally more stable than HgCdTe.[4] Due to the weak Hg-Te bonding in the Hg-containing alloys, these substrates are easily severely disrupted during overlayer deposition.[5] By studying metal interfaces with the related binaries, we can gain insight into the role of the weak Hg-bonding in the alloys HgCdTe and HgZnTe during metal contact formation.

We reported during last year our findings that Al, highly reactive with Te, yields a significantly more extensive reacted region on CdTe than on HgCdTe, suggesting that the severe and rapid Hg loss at the Al/HgCdTe interface inhibits further reaction.[6] The Al overlayer thus presents a case where a higher degree of intermixing is possible in absence of Hg. Reaction at the Al/CdTe interface was also found to be significantly more extensive than for the corresponding Al/ZnTe interface. We report further studies comparing interfacial morphology for In, Ag, and Pt overlayers on CdTe and ZnTe. The four metals in this study provide a range of reactivities with the substrates. Relevant bulk thermodynamic heats of formation and heats of alloying for these metal/semiconductor interfaces provide a guide for predicting the most likely chemical interactions. Al [$\Delta H_f(Al_2Te_3)$ = -76.1 kcal/mol] is expected to be highly reactive with Te; and In and Ag less reactive [for example: $\Delta H_f(In_2Te_3)$ = -45.8 kcal/mol and $\Delta H_f(Ag_2Te)$ = -8.6 kcal/mol].[7]

Calculations based on the semiempirical model of Miedema[8] predict for Pt a large driving force for cation (Cd or Zn) movement into the overlayer [ΔH_{sol}(Cd;Pt) = -24.4 kcal/mol and ΔH_{sol}(Zn;Pt) = -30.0 kcal/mol]. For Al, In, and Ag, minimal alloying behavior is expected. The heats of formation of CdTe and ZnTe are very similar [ΔH_f(CdTe) = -24.1 kcal/mol and ΔH_f(ZnTe) = -28.5 kcal/mol][7] and therefore similar chemical behavior is expected for these metal overlayers on both substrates.

The salient features of the observed chemistry at these interfaces are described, and results are compared to metal/HgCdTe interface formation, where we consider the influence of Hg loss on the resulting chemistry and overlayer morphology that has been observed. Our objective is also to correlate observed interfacial morphology with Fermi level movement within the bandgap. We consider possible explanations for the observed Fermi level movement with coverage, focussing on the metal-induced gap states (MIGS) model[9] and what would be expected for a defect mechanism to operate. Formation of defects is likely in view of the chemical reactions and intermixing seen.

II. EXPERIMENTAL SECTION

Experiments were performed on Beamline I-1 and Beamline I-3 (Old and New Grasshopper monochromators) at the Stanford Synchrotron Radiation Laboratory (SSRL). Photon energies were chosen to provide a range of surface sensitivities (electron escape depth, λ ~5 - 7 Å and ~10 - 20 Å). Experiments were also performed using a He discharge lamp for UPS studies (He I and He II, 21.2 and 40.8 eV). The kinetic energy of the photoemitted electrons was analyzed using a double-pass cylindrical mirror analyzer (CMA). In some cases (Al/CdTe, Pt/CdTe and Pt/ZnTe), low-energy electron diffraction (LEED) was performe 'n order to monitor surface crystallinity during overlayer growth.

Bulk single crystal bars of *p*-type CdTe (cross-sectional area 5 x 5 mm^2) and *p*-type ZnTe (2 x 2 mm^2, obtained from Cleveland Crystals, Inc.) were cleaved in vacuum (base pressure < 1 x 10^{-10} torr) to produce atomically clean (110) surfaces . Sequential metal depositions were performed

by evaporation from a tungsten filament, with rate calibrations performed using a quartz microbalance. Throughout the following, metal coverage is given in terms of a monolayer (ML), equivalent to the surface density of atoms on the (110) faces of CdTe and ZnTe (6.74×10^{14} and 7.60×10^{14} atoms/cm^2, respectively).

For the metal/ZnTe studies, the samples used were cut from the same bulk grown material. For the *p*-CdTe studies here, Al, Ag, and Pt evaporations were all performed on the same sample. In overlayers were studied on a second *p*-CdTe crystal. On ZnTe, the as-cleaved position of the Fermi level relative to the valence band maximum (VBM) was remarkably reproducible for all four cleaves (yielding Fermi level positions 0.5, 0.4, 0.4, and 0.35 eV above the VBM for the In, Al, Ag, and Pt cleaves, respectively). This consistency is attributed to the excellent, mirror-like surfaces, with a few faint lines indicating steps, obtained from these ZnTe samples. Cleave quality on the CdTe samples was not as consistent (E_f - E_{VBM} values 0.75, 0.5, 0.65, 0.45 eV for the In, Al, Ag, and Pt cleaves, respectively). For CdTe, the initial E_f - E_{VBM} has been found, for several cleaves, to be dependent on cleave quality. The method used to determine E_f - E_{VBM} is described later.

III. RESULTS

A. Interfacial Chemistry

1. In overlayers

In proves to be the least reactive of the four metals studied, on both CdTe and ZnTe. Only a slight initial reaction of In on CdTe is observed, and no direct evidence is seen for reaction on ZnTe, with only metallic In observed. Figure 1 shows the growth of In 4d core level emission with increasing In coverage on (a) CdTe and (b) ZnTe. The insets show evolution of this emission for the lower coverages (up to 1.5 monolayers). On both CdTe and ZnTe, emission from metallic In 4d is seen at the lowest coverage and grows in intensity with metal deposition, with its binding energy relative to the Fermi level remaining constant up to the highest coverages. On CdTe at the lowest coverage [see inset Figure 1(a)] a small additional In 4d component due to reacted In is also

seen, emerging at approximately 1.15 eV lower kinetic energy (higher binding energy) than the metallic contribution. This chemically shifted component stops growing in intensity above 0.3 ML coverage. On ZnTe, no shifted In 4d component appears with deposition, indicating that only metallic In is formed.

Surface-sensitive emission from the cation core levels Cd 4d or Zn 3d and the anion core level Te 4d are shown in Figure 2 for (a) CdTe and (b) ZnTe. These signals attenuate with increasing coverage of In as the overlayer grows. On CdTe, both the Te 4d and Cd 4d substrate emission shows no shifted components with In deposition, and changes in width (FWHM) are negligible ($\leq$ 0.06 eV) for both. For Al overlayers, which do exhibit strong reaction with Te on both CdTe and ZnTe, no binding energy shift is seen for reacted Te, however broadening is observed in the Te 4d emission (FWHM increases ~ 0.4 eV) and the spin orbit splitting becomes smeared.[6] For the limited chemical interaction seen here for In/CdTe, any such changes might not be observed. On ZnTe, an initial decrease in the Zn/Te ratio at the surface is observed which might indicate some degree of initial outdiffusion of Te. The Zn/Te ratio remains constant beyond 0.7 ML coverage, however, which suggests that any Te initially segregating to the suface becomes covered up as the metal overlayer grows. Similar behavior is seen for In/CdTe. By 0.1 ML coverage, emission above the valence band maximum (VBM) becomes apparent on both CdTe and ZnTe. This and the slow overall attenuation of the Cd 4d and Zn 3d substrate signals with coverage give evidence that overlayer growth occurs by formation of metal islands on the surface of both substrates.

Since no appreciable changes in the lineshape of the cation core level emission occurs that might indicate chemical interaction with the overlayer occurs, this signal belongs to the substrate and energy shifts in the the Cd 4d and Zn 3d core levels may be used to track shifts in the Fermi level within the gap due to band bending, as described later.

2. Al overlayers

A study of the Al/CdTe and Al/ZnTe interfaces has been previously reported[6], and the important features are summarized here. A strong Al - Te reaction is seen for both substrates, with Al 2p emission showing a shifted component due to reacted Al at ~2.5 eV higher binding energy

than metallic Al 2p. Al emission first emerges in reacted form, and metallic core level emission is not seen until near 40 ML on CdTe and near 7 ML on ZnTe. At these higher coverages, a surface-segregated Al - Te reacted layer remains on the overlayer surface. On CdTe, surface-sensitive emission from the Cd 4d core level attenuates much more rapidly than that for Te 4d, indicating that Cd is not incorporated into the Al overlayer. The substrate signals attenuate at a slower rate than expected for formation of a uniform, abrupt interface, and persistance of LEED until ~10 ML coverage indicates that the overlayer grows inhomogenously, with initial islanding, and intermixing of components. Significantly, for both Al/CdTe and Al/ZnTe, Fermi-level emission is not established and a metallic Al 2p component is not seen until well after band bending has stabilized. No emission above the VBM is seen for Al on *p*-CdTe until 29.8 ML and on *p*-ZnTe until 7.4 ML, giving no indication of any metallic phase in contact with the substrate surface. This point will be discussed later.

3. Ag overlayers

On CdTe and ZnTe, Ag is found to be moderately reactive with Te, in comparison to In overlayers. Although Ag is predicted to be the least reactive of these four metals[7], a Ag - Te reaction has been seen on CdTe[3] and we see clear evidence here for a Ag-Te reaction on ZnTe. Figure 3 shows surface-sensitive emission from (a) the Zn 3d and (b) the Te 4d core levels for the Ag/*p*-ZnTe interface. As metal is deposited, the signal from these substrate core levels attenuates as the overlayer grows. A shifted component of Te 4d emission emerges with increasing coverage at ~0.6 eV higher kinetic energy (lower binding energy) than the substrate Te 4d signal on ZnTe. This shifted component emerges with a binding energy relative to the Fermi level of -39.7 eV, which is approximately 1.5 eV lower than that expected for elemental (dissociated) Te, and is therefore consistent with reacted Te. The binding energy of the reacted Te here is very similar to that reported for Ag/CdTe[3]. The reacted component is especially apparent at the 8.7 ML coverage in Figure 3(b) as a shoulder on the high kinetic energy side of each component of the Te 4d doublet.

On ZnTe, initially the Zn 3d and Te 4d signal intensities attenuate at the same rate, until 2.2 ML coverage, when the Te signal begins to level off. The Zn 3d emission also begins to show slight broadening (≤ 0.1 eV), indicating a change in the chemical environment of the Zn, possibly due to some Zn intermixing with the overlayer. The slow attenuation of the Zn signal throughout indicates the overlayer grows inhomogenously. By a coverage of 0.4 ML on both CdTe and ZnTe, some emission extends above the VBM, providing evidence of initial formation of metallic clusters. At 0.7 ML on ZnTe broadening of the Te 4d due to reaction becomes apparent, and by 8.7 ML the reacted component makes up ~20% of the total Te 4d signal.

4. Pt overlayers

Pt exhibits a complex overlayer morphology, with movement of Cd and Zn into the overlayer and simultaneous formation of dissociated Te. The overlayer grows inhomogenously, with islanding and intermixing of components. Minimal reaction with Te is expected[7]; however, a strong driving force for alloying with the cations Cd or Zn is predicted.[8] Figure 4 shows emission from the cation core levels Cd 4d and Zn 3d for (a) CdTe and (b) ZnTe with increasing coverage of Pt. A shifted component in both Cd 4d and Zn 3d emission to higher kinetic energy (lower binding energy) occurs with Pt deposition, resulting from dissociation of the cation from the substrate and its movement into the overlayer. The shifts in the core level positions for both Cd 4d and Zn 3d are consistent with calculated binding energy shifts for Cd and Zn alloyed with Pt using ΔH_{sol} values[8] as described in Ref. 10. The shift is not abrupt and emission is broad, reflecting continuous changes in the surface Cd or Zn environment as intermixing proceeds. Formation of dissociated Te occurs simultaneously (observed using more bulk-sensitive XPS). The shift for Cd alloyed with Pt has been seen experimentally also for Pt/HgCdTe[11].

The overlayer grows in a non-abrupt manner on both CdTe and ZnTe. The LEED pattern for Pt/CdTe persists beyond 4.6 ML Pt coverage and disappears at 9.5 ML. On ZnTe, the LEED pattern is still seen (very diffuse) at 10.8 ML and disappears at 20 ML. Emission above the VBM to the Fermi level for both CdTe and ZnTe is seen at 0.6 ML, giving evidence for metal islanding at

the low coverages. Detectable broadening of the Cd 4d and Zn 3d core levels occurs at 0.6 ML for ZnTe and 1.2 ML for CdTe, indicating the onset of alloying, when substrate disruption begins.

B. Band Bending

The movement of the Fermi level relative to the VBM from its initial as-cleaved position (before any metal is deposited) as metal is successively deposited is obtained by measuring shifts in the binding energies of the cation Cd 4d and Zn 3d core levels. The binding energies of these cation cores relative to the VBM are known accurately from ARPES measurements, which yield a sharper VBM cutoff than angle-integrated PES: the VBM lies 10.25 ± 0.05 eV above Cd $4d_{5/2}$ in CdTe and 9.75 ± 0.05 eV above Zn 3d in ZnTe.[12] The cation core level positions are determined for the as-cleaved surface, and movement of the VBM (relative to E_f) corresponding to band bending is tracked as energy shifts in these cores, until any chemically shifted components obscure the substrate signal. The final Fermi level positions are thus obtained. We give the uncertainty in E_f - E_{VBM} as ± 0.1 eV, which reflects the accuracy with which the absolute binding energy of the cation cores and the metal Fermi level cutoff used as a reference can be measured (each to within 0.05 eV). Any inaccuracy in the method of determining the *absolute* binding energies, however, will be reproduced for all the Φ_{bp} measured, so that the *relative* separation between the E_{fi} for the different metals on each semiconductor can be known well within ± 0.1 eV.

The measured Fermi level position relative to the valence band maximum, E_f - E_{VBM}, for *p*-CdTe and *p*-ZnTe is indicated in Figure 5 as a function of metal coverage for In, Al, Ag, and Pt overlayers. The same energy scale is used for both semiconductors, with the bandgaps of CdTe and ZnTe given as 1.5 eV and 2.2 eV, respectively. Schottky barriers are formed for all four metals on both semiconductors, with E_f moving from its initial as-cleaved position (before any metal is deposited) towards the conduction band upon metal deposition. A narrow range of final Fermi level positions $E_{fi} = \Phi_{bp}$ within the gap is observed for CdTe, with values from 0.9 to 1.05 ± 0.1 eV, and for ZnTe values from 0.65 to 1.0 ± 0.1 eV. The average final E_{fi} for CdTe and ZnTe lie at roughly the same position relative to their VBM's (with E_{fi} values for ZnTe lying below

midgap). The formation of Schottky barriers on *p*-CdTe here is in contrast to previous studies on *n*-CdTe cleaved in vacuum in which ohmic behavior is reported for Al, In, and Ag.[22,23]

The band bending *vs.* coverage diagrams show that the final Fermi level positions for these four metals retain nearly the same relationship for both CdTe and ZnTe, with E_{fi} for Al and In lying higher than E_{fi} for Ag and Pt on both semiconductors, by ~0.1 eV on CdTe and ~0.3 eV on ZnTe. Additionally, for Al/*p*-CdTe and Ag/*p*-ZnTe, the Fermi level exhibits a bowing behavior, moving higher towards the CBM and then decreasing to its final position near ~10 ML coverage for Al/*p*-CdTe and ~2 ML coverage for Ag/*p*-ZnTe. These observations are discussed further below.

IV. DISCUSSION

A. Interfacial Chemistry: Comparison with metals on HgCdTe

Here we compare observed interfacial chemistry and morphology for In, Ag, and Pt overlayers on CdTe, ZnTe, and HgCdTe.

Bulk thermodynamic heats of metal telluride formation considered along with heats of alloying for the cations in the metal overlayer in general have been found to correlate with the observed interfacial reactivity and provide a useful guide for predicting interface behavior.[5,19] In forms several tellurides of intermediate reactivity, of which the most stable is In_2Te_3 (for ΔH_f normalized per mole metal atoms).[7] Considering only bulk heats of telluride formation, it is expected that the extent of Te reaction observed would decrease in the sequence Al, In, Ag. However, significantly more Ag-Te reaction is observed on CdTe and ZnTe than would be expected from these considerations alone. Interface formation for Ag may be influenced to some extent by the heat of solution of the cation Cd or Zn into the Ag overlayer, which is small but negative in comparison to In.[13] In such a case, some cation movement into the overlayer might facilitate further Te reaction.

Whereas Al is highly reactive with both binaries CdTe and ZnTe[6], In shows only slight reaction with CdTe and no evidence for In reaction on ZnTe is seen. However both of these metals behave similarly on HgCdTe: below 2 Å coverage In reacts with Te, forming a reacted layer at the

interface. With further deposition, unreacted (metallic) In grows on top of this layer, with a surface-segregated Te-rich layer moving to the overlayer surface.[15] In Ref. 14, it can be seen that at a 10 Å coverage of In on HgCdTe, roughly half of the In signal is due to a reacted contribution. This behavior of In on the alloy differs from what is seen on the binaries, where little or no evidence for In reaction is seen, as discussed above. The greater substrate disruption on HgCdTe is also apparent in the degree of Te outdiffusion. For In/HgCdTe[15] the Te concentration at the surface increases upon initial metal deposition due to Te reaction and outdiffusion and remains higher than at the cleaved surface throughout, resulting in a continuously decreasing Cd/Te ratio in the near-surface region. On CdTe and ZnTe, in contrast, the cation and Te signals attenuate with coverage at about the same rates at the higher coverages. For the case of In overlayers, it appears that In-Te reaction is enhanced on HgCdTe due to Hg loss, yielding an interfacial morphology very similar to the highly reactive Al overlayer.

Ag behaves differently at interfaces with HgCdTe, CdTe, and ZnTe. The Ag-Te reaction seen for the binaries differs significantly from what is seen for Ag/HgCdTe[16], where no reaction has been seen, with Ag instead diffusing 100 to 1000 Å into the HgCdTe bulk. The Ag/HgCdTe interface may be dominated by the disruption due to Hg depletion, perhaps by providing a possible Ag-Hg replacement mechanism by which Ag is able to diffuse umimpeded far into the bulk, as has been proposed.[16]

In contrast to Al, In, and Ag overlayers where reactivity with Te is expected, interfaces with Pt are dominated by the cation reaction with the overlayer, with movement of Cd or Zn into the overlayer and formation of dissociated Te, and significant disruption is seen for all three substrates CdTe, ZnTe, and HgCdTe. However, due to the substantial Hg loss which occurs at Pt/HgCdTe[11], this interface is much more severely disrupted at comparable metal coverages. By 0.6 ML coverage on HgCdTe, 25% of the Hg has been depleted, and by 2 ML 50-90%. This severe Hg depletion leads to a collapse of the lattice: deep disruption and loss of surface order are indicated by the early disappearance of the LEED pattern below 1 ML metal coverage.[11] In contrast, the persistance of LEED at higher coverages on CdTe and ZnTe indicate the retention of

surface order over large portions of the surface at coverages ~5-10 ML (the coherence length for LEED is on the order of 50-500 Å). For Pt, similar interfacial reaction is seen for both CdTe and ZnTe. The onset of Cd and Zn alloying with Pt, indicated by a shifted contribution of Cd 4d and Zn 3d emission at higher kinetic energy (lower binding energy), occurs at 1.2 ML on CdTe, and at 0.6 ML on ZnTe . This similarity in behavior suggests that the driving force for reaction at the surface in this case dominates any differences between the CdTe and ZnTe, in comparison to HgCdTe.

B . Band bending

In this section, the models of Schottky barrier formation consistent with the observed band bending *vs.* coverage and the final barrier heights for In, Al, Ag, and Pt overlayers on *p*-CdTe and *p*-ZnTe shown in Figure 5 are considered in detail.[17] The prominent features of the observed Fermi level movement in the bandgap (1.5 eV for CdTe, 2.2 eV for ZnTe) are discussed in light of predictions of the MIGS model and what would be expected for a defect mechanism to operate. The preliminary results presented here for these four metals offer interesting comparisons between these two II-VI semiconductors since similar chemical interactions are exhibited by both. We can also draw upon present understanding of III-V systems such as GaAs.

The simple dependence of the barrier height Φ_{bp} on the metal work function Φ_m predicted by the Schottky model, $\Phi_{bp} = E_g - (\Phi_m - \chi_s)$, is not seen in the present data. Rather, the narrow range of E_{fi} within the gap is more consistent with either the metal-induced gap states (MIGS) model[29], or a defect mechanism. The narrow range here differs with earlier work[1,23] which found a wider range of barrier heights Φ_{bn} on *n*-CdTe, including ohmic behavior for In, Al, and Ag as mentioned above. In Figure 6, the final Fermi level position in the gap is plotted *vs.* both the polycrystalline work function[24] and the Miedema electronegativity[8]. Included are barrier heights $\Phi_{bp} = E_{fi}$ from Ref. 3 measured using PES for Au and Cu on *p*-CdTe, and also E_{fi} for Ag and Cu[3] and Pd[21] on *n*-CdTe (shown as solid symbols).[25] No strong metal dependence is evident. For instance, the index of interface behavior, $S = - d\Phi_{bp}/d\Phi_m$, a parameter which describes the

"pinning strength" of the semiconductor[26,27], derived from the present data using the Miedema electronegativity values[8] via linear regression yields for CdTe S = 0.06. Including also E_{fi} values from Refs. 3 and 21 for CdTe gives S = 0.08, and it should be noted that for CdTe, any sensitivity to the metal that might be exhibited in Figure 6 is of the same degree as that observed for metal/GaAs systems.[28] For ZnTe, a slope S = 0.18 is derived. As Figure 6 shows, ZnTe exhibits a wider range in E_{fi} values than CdTe which does not strictly correlate with the metal electronegativity. The involvement of other mechanisms may be suggested by the present data, although additional results for other metals on ZnTe are necessary before any definite conclusions can be drawn.

The MIGS model, without corrections for metal electronegativity effects, would predict a final surface Fermi level position above the VBM at ~0.85 for CdTe and ~0.84 eV for ZnTe that would be the same for all metal interfaces.[9] The range of Fermi level positions found for these metals include the calculated values; however, the MIGS mechanism alone cannot account for the observed range in Φ_{bp} values of ~0.15 eV for CdTe and ~0.35 eV for ZnTe. In addition, as Tersoff argues[9], E_{fi} for two semiconductors are expected to be separated by an amount equivalent to their valence band offset (ΔE_v). From Tersoff's calculated values given above, a valence band offset $\Delta E_v = 0.01 \pm 0.2$ eV is predicted. The CdTe - ZnTe valence band offset has recently been experimentally determined as $\Delta E_v = 0.18 \pm 0.06$ eV using ARPES, as described in Ref. 12, with the ZnTe VBM lying above that of CdTe, which is within the range of the calculated value

In considering differences between barrier heights measured for CdTe and ZnTe, we focus on metals of similar electronegativity. For CdTe, E_{fi} for In, Al, and Ag are concentrated near the same value ~1.0 eV. For ZnTe, however, the spread in E_{fi} (a range of 0.35 eV) is not suggestive of a simple correlation with ΔE_v, neither is it suggestive of metal dependence effects (unless the value for Pt is omitted). Figure 6 shows that E_{fi} for Al, Ag, and Pt are indeed found to lie higher on CdTe than on ZnTe, by ~0.2 eV. However, any simple correlation between these barrier height differences seen for the same metal on *p*-CdTe and *p*-ZnTe and their valence band offset neglects the details of the interfacial interactions occurring, including chemical reaction, alloying, and island

formation. Interface morphology is an important factor influencing the final Fermi level position for metal/GaAs systems.[30] As discussed for the Al/CdTe and Al/ZnTe interfaces, no evidence of overlayer metallicity, from either metallic core level emission or any emission from states above the VBM, is seen until well after the Fermi level position has stabilized on both CdTe and ZnTe. Since the MIGS mechanism requires that the overlayer exhibit metallicity[30], this mechanism appears to be ruled out in these studies for the case of the highly reactive Al.

MIGS are expected to dominate at ideal, nondisruptive interfaces.[30] The In interfaces are then of special interest, since they show the least reactivity of the metals considered here. However, the final barrier heights for In on CdTe and ZnTe are the same, 1.0 ± 0.1 eV. Tersoff argues[9,31] that for II-VI semiconductors, the relationship $\Phi_{bp} = \Delta E_v$ might not apply, since due to the smaller dielectric constants the MIGS might be unable to pin as effectively as on III-V semiconductors.[29,32] A larger dependence of Φ_{bp} on the metal should then be exhibited, however, which is not seen here for CdTe and ZnTe, relative to III-V semiconductors such as GaAs. It would be of interest to establish whether differences in band bending behavior occur for In overlayers deposited at low temperature, where the surface mobility of adatoms is reduced and metal island formation is inhibited. For In and Ag on GaAs, low temperature leads to more uniform metal overlayer growth and a final barrier height that is consistent with MIGS predictions.[30]

The reactions and intermixing seen for Al, Ag, and Pt here on CdTe and ZnTe indicate that these interfaces are certainly not ideal and raise the possibility that defects might be involved in barrier formation, with the heat of reaction with the semiconductor providing energy for generation of defects. For strongly clustering nonreactive overlayers (here, In overlayers), the heat of cluster condensation of the metal[33] can also create defects. For the case of Al, extensive reaction resulting in a thick intermixed region near the surface is observed. For Pt, significant cation and Te dissociation from the substrate also occurs. Defect formation would be expected to be more rapid for these more reactive cases, and the more rapid band bending observed for these cases is consistent with this, except for the case of Al/CdTe which is considered further below.

The possibility that defects influence Schottky barrier formation on CdTe has been considered by others.[1,18] In considering which defects are likely to be involved, we focus on those involving Te, in view of the Te outdiffusion and/or reaction frequently observed at metal/CdTe interfaces.[3] Calculations of bulk defect energies in the HgTe - CdTe system from the work of Kobayashi *et al.*[34] offer support for this possibility. From their work, an intrinsic defect that might be involved in Fermi level movement in CdTe is the Te_{Cd} antisite, with a calculated energy ~1eV above the VBM, which could account for the observed narrow spread of E_{fi} values on CdTe seen here and by others.[2] The Te vacancy is also predicted to be a shallow double donor in CdTe[35], however the Te_{Cd} antisite is considered more likely, from Ref. 34. For metal/GaAs systems, the involvement of more than one type of defect in Schottky barrier formation can explain spreads of ~0.25 - 0.3 eV in barrier heights seen for different metals.[36] A similar mechanism may operate here. Other defects that may influence Fermi level movement might involve Cd, considering that the Cd_{Te} antisite and Cd vacancy energy levels lie closer to the VBM.[34,35,37] Deep levels observed with photoluminescence (PL) occurring at ~0.9 and ~1.1 eV in p-CdTe that has been chemically etched have been associated with alterations in stoichiometry due to etching.[38] Similar PL transistions (at ~0.8 and 1.1 eV) have also been observed at In and Au interfaces with CdTe and a correlation between these transitions and observed stages in Fermi level movement within the gap for In/CdTe has been suggested.[39,40] These works provide possible evidence for associating the observed final E_f positions on CdTe with deep levels due to defects. Comparison with ZnTe is hampered by lack of available information on defect levels for this system, however it is reasonable that similar defects would be involved here.

In Figure 5, the movement of E_f exhibits a bowing behavior for Al/*p*-CdTe and Ag/*p*-ZnTe. An overshoot in E_f movement is also seen for metal/*p*-GaAs systems and is attributed to adatom donation of electrons to acceptor states. However, this effect is generally observed only at low temperature, where metal islanding and reaction is inhibited, resulting in more uniform overlayer growth, and is usually finished below about 1 ML, at the onset of overlayer metallicity in these systems. For Al/CdTe, overlayer growth does not occur in an abrupt, uniform manner.

Additionally, E_f does not decrease to its final position for Al/CdTe until near ~10 ML and for Ag/ZnTe until ~ 2 ML. This suggests that a different mechanism is involved here. One possibility was proposed by Ludeke[41] to explain E_f bowing occurring over several ML for Ag/GaAs which depends upon interaction between the defects or impurities responsible for E_f movement in the gap at submonolayer coverages and the developing metallic overlayer at higher coverages. However, for the Al/*p*-CdTe interface evidence for any metallic character in the overlayer in the coverage range where bowing occurs is not observed. For Al, the observed overshoot might be explained by some initial doping of the lattice by indiffusion of Al, which is a donor in CdTe.[37] Some initial indiffusion is certainly a possibility to be considered, given the slow substrate signal attenuation with Al deposition and the degree of intermixing observed. There is strong evidence that such doping by the deposited metal occurs also at metal/HgCdTe interfaces.[5,20]

V. CONCLUSIONS

In summary, we have described interfacial chemistry and band bending behavior for Al, In, Ag, and Pt overlayers on vacuum-cleaved *p*-CdTe and *p*-ZnTe (110). A range of metal-substrate reactivities have been considered: Al reacts strongly with Te, Ag moderately, and In minimally, with no evidence seen for In reaction on ZnTe. Pt exhibits strong alloying behavior with both Cd and Zn. These results for the binaries are compared to metal/HgCdTe interface formation, where it is found that Hg loss can significantly influence the extent of reaction and/or intermixing for these overlayers, with resulting disruption either inhibiting or facilitating chemical interaction. All four metals are found to yield Schottky barriers on CdTe and ZnTe, with a narrow range of final Fermi level positions, $E_{fi} = E_f - E_{VBM}$, observed on CdTe, from 0.9 to 1.05 ± 0.1 eV, and on ZnTe from 0.65 to 1.0 ± 0.1 eV, consistent with either the MIGS model or a defect mechanism for Fermi level movement. For the highly reactive Al, no evidence for the overlayer metallicity required for MIGS to operate is seen on CdTe or ZnTe until after band bending has stabilized. Reaction and intermixing for Al, Ag, and Pt overlayers on CdTe and ZnTe indicate these interfaces are not ideal.

A defect mechanism for Fermi level movement provides a consistent explanation for the final Fermi level positions observed.

ACKNOWLEDGEMENTS

*Work supported by DARPA under Contract No. N00014-86-K0854.

REFERENCES

a) Stanford Ascherman Professor of Engineering

1. I. M. Dharmadasa, W. G. Herrenden-Harker, and R. H. Williams, Appl. Phys. Lett. **48**, 1802 (1986).
2. Tabulations in Ref. 3.
3. D. J. Friedman, I. Lindau, and W. E. Spicer, Phys. Rev. B **37**, 731 (1988).
4. A. Sher, A.-B. Chen, W. E. Spicer, and C.-K. Shih, J. Vac. Sci. Technol. A **3**, 105 (1985).
5. D. J. Friedman, G. P. Carey, I. Lindau, and W. E. Spicer, J. Vac. Sci. Technol. A **5**, 3190 (1987).
6. A. K. Wahi, G. P. Carey, T. T. Chiang, I. Lindau, and W. E. Spicer, J. Vac. Sci. Technol. A **7**, 494 (1989).
7. K. C. Mills, *Thermodynamic Data for Inorganic Sulfides, Selenides, and Tellurides* (Butterworths, London, 1974).
8. A. R. Miedema, P. F. de Châtel, and F. R. de Boer, Physica B **100**, 1 (1980).
9. J. Tersoff, Phys. Rev. Lett., **56**, 2755 (1986).
10. J. Nogami, T. Kendelewicz, I. Lindau, and W. E. Spicer, Phys. Rev. B **34**, 669 (1986).
11. D. J. Friedman, G. P. Carey, I. Lindau, and W. E. Spicer, Phy. Rev. B **35**, 1188 (1987).
12. C. K. Shih, A. K. Wahi, I. Lindau, and W. E. Spicer, J. Vac. Sci. Technol. A **6**, 2640 (1988).
13. Calculation of the heat of solution of Zn at infinite dilution in metal M using the semiempirical model of Miedema (Ref. 8) gives values ΔH_{sol}(Zn;M) of -4.3 kcal/mol for Ag and +2.4 kcal/mol for In. Calculated values ΔH_{sol}(Cd;M) are tabulated in Ref. 5.
14. G. D. Davis, W. A. Beck, D. W. Niles, E. Colavita, and G. Margaritondo, J. Appl. Phys. **60**, 3150 (1986).
15. G. D. Davis, N. E. Byer, R. A. Riedel, and G. Margaritondo, J. Appl. Phys. **57**, 1915 (1985).
16. D. J. Friedman, G. P. Carey, C. K. Shih, I. Lindau, W. E. Spicer, and J. A. Wilson, J. Vac. Sci. Technol. A **4**, 1977 (1986).

17. A. K. K. Miyano, P. Carey, T. T. Chiang, I. Lindau, and W. E. Spicer, to be published, J. Vac. Sci. Technol. A.

18. L. J. Brillson, C. F. Brucker, N. G. Stoffel, A. Katnani, R. Daniels, G. Margaritondo, Physica **117**B & **118**B, 848 (1983), and refs. therein.

19. J. F. McGilp and I. T. McGovern, J. Vac. Sci. Technol. B **3**, 1641 (1985).

20. G. P. Carey, A. K. Wahi, D. J. Friedman, C. E. McCants, and W. E. Spicer, J. Vac. Sci. Technol. A **7**, 483 (1989).

21. G. P. Carey, Ph. D. Thesis, Stanford University, 1988.

22. M. H. Patterson and R. H. Williams, J. Cryst. Growth **59**, 281 (1982).

23. R. H. Williams and M. H. Patterson, Appl. Phys. Lett. **40**, 484 (1982).

24. H. B. Michaelson, J. Appl. Phys. **48**, 4729 (1977).

25. Values from Refs. 3 and 21, in which a binding energy of Cd $4d_{5/2}$ relative to the VBM of 10.3 eV ± 0.05 is used, have here been shifted by +0.05 eV.

26. S. Kurtin, T. C. McGill, and C. A. Mead, Phys. Rev. Lett. **22**, 1433 (1969).

27. M. Schlüter, Phys. Rev. B **17**, 5044 (1978).

28. R. Cao *et. al*, submitted for publication.

29. J. Tersoff, Phys. Rev. Lett. **52**, 465 (1984).

30. W. E. Spicer, R. Cao, K. Miyano, C. McCants, T. T. Chiang, C. J. Spindt, N. Newman, T. Kendelewicz, I. Lindau, E. Weber, and Z. Lilienthal-Weber, in *Metallization and Metal-Semiconductor Interfaces*, NATO ASI Conference Series, edited by I. P. Batra (Plenum Press, New York, 1989).

31. J. Tersoff, J. Vac. Sci. Technol. B **3**, 1157 (1985).

32. S. G. Louie, J. R. Chelikowsky, and M. L. Cohen, Phys. Rev. B **15**, 2154 (1977).

33. A. Zunger, Phys. Rev. B **24**, 4372 (1981).

34. A. Kobayashi, O. F. Sankey, and J. D. Dow, Phys. Rev. B **25**, 6367 (1982).

35. M. S. Daw, D. L. Smith, C. L. Swarts, and T. C. McGill, J. Vac. Sci. Technol. **19**, 508 (1981).

36. W. E. Spicer, Z. Liliental-Weber, E. Weber, N. Newman, T. Kendelewicz, R. Cao, C. McCants, P. Mahowald, K. Miyano, and I. Lindau, J. Vac. Sci. Technol. B **6**, 1245

(1988).

37. K. Zanio, *Semiconductors and Semimetals, Vol 13 Cadmium Telluride*, edited by R. K. Willardson and A. C. Beer (Academic Press, New York, 1978).

38. Z. Sobiesierski, I. M. Dharmasa, and R. H. Williams, Appl. Phys. Lett. **53**, 2623 (1988).

39. J. L. Shaw, R. E. Viturro, L. J. Brillson, D. Kilday, and G. Margaritondo, J. Elect. Mat. **17**, 149 (1988).

40. J. L. Shaw, R. E. Viturro, L. J. Brillson, and D. LaGraffe, J. Vac. Sci. Technol. A **7**, 489 (1989).

41. R. Ludeke, G. Jezequel, and A. Taleb-Ibrahimi, J. Vac. Sci. Technol. B **6**, 1277 (1988).

Figure Captions

Figure 1. Surface-sensitive photoemission spectra showing the growth of metallic In 4d core level emission with increasing In coverage on (a) CdTe and (b) ZnTe. On CdTe an additional In 4d component is seen at the lowest coverages (shown in inset), chemically shifted to higher binding energy (lower kinetic energy) than the metallic contribution. Metal coverage is given in monolayers (ML).

Figure 2. Photoemission from the substrate core levels for In overlayers on (a) CdTe and (b) ZnTe. Cation Cd 4d or Zn 3d and anion Te 4d emission is shown with increasing metal coverage. The lack of appreciable lineshape changes in this emission is an indication of minimal chemical interaction between overlayer and substrate. Shifts may then be attributed to band bending. Dashed line indicates peak position for as-cleaved surface.

Figure 3. (a) Zn 3d and (b) Te 4d core level emission for Ag/ZnTe with increasing Ag coverage. Ag-Te reaction is indicated by an additional component of Te 4d emission shifted to higher kinetic energy than the substrate signal. At 8.7 ML (indicated in bold), the shifted component due to reacted Te contributes ~20% of the total Te 4d signal.

Figure 4. Cd 4d and Zn 3d cation core level emission for Pt overlayers on (a) CdTe and (b) ZnTe with increasing coverage of Pt. A shift occurs to higher kinetic energy resulting from dissociation of the cation from the substrate and its movement into the overlayer. Te dissociation occurs simultaneously.

Figure 5. The position of the Fermi level relative to the VBM, $E_f - E_{VBM}$, for (a) *p*-CdTe (E_g = 1.5 eV) and (b) *p*-ZnTe (E_g = 2.2 eV) as a function of metal coverage for Al, In, Ag, and Pt overlayers. The same energy scale is used for both.

Figure 6. The final Fermi level position in the gap relative to the VBM, E_{fi}, from Figure 5, for metals on CdTe and ZnTe *vs.* both polycrystalline work function and the Miedema electronegativity. See text for discussion.

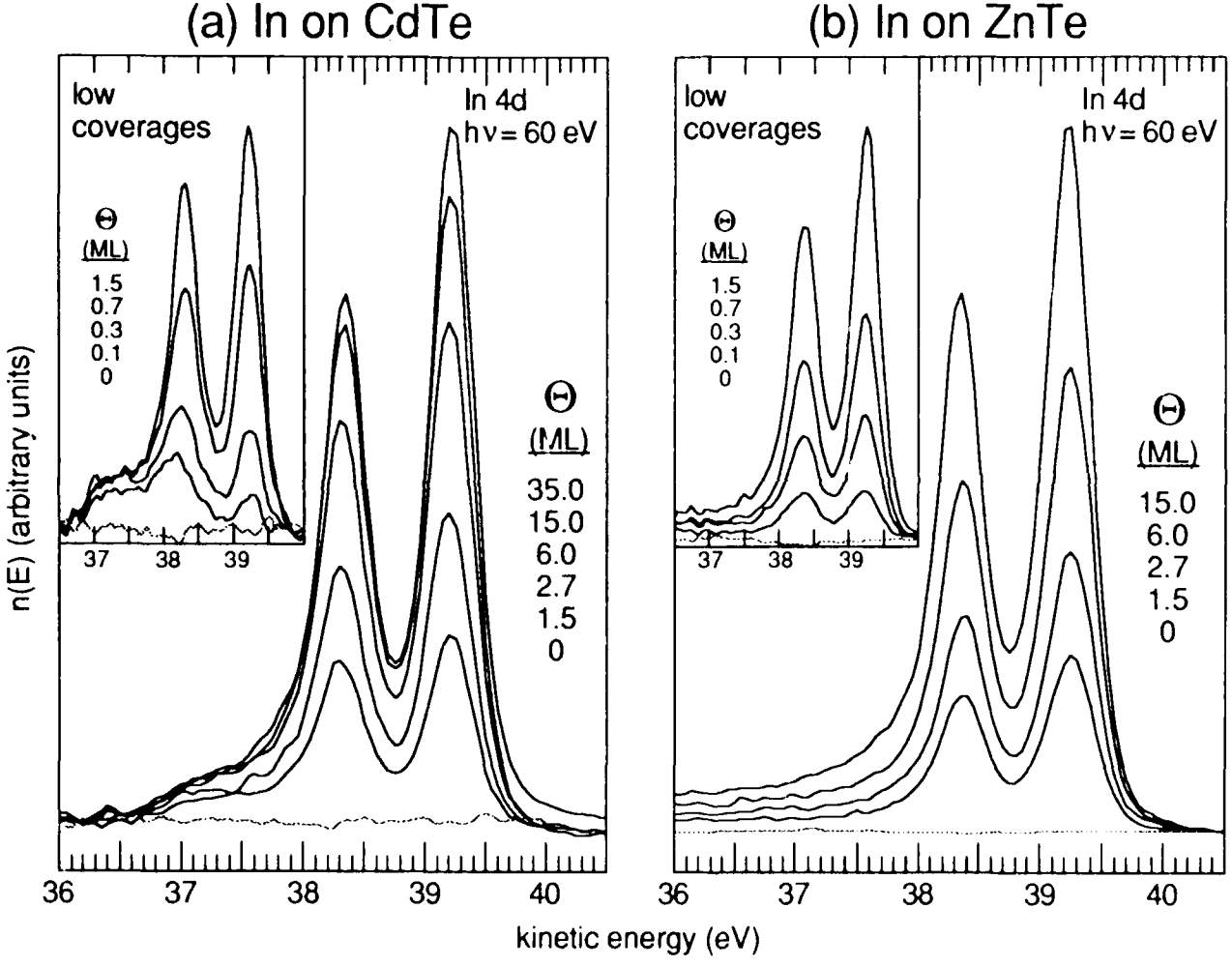
(a) In on CdTe
(b) In on ZnTe
low
coverages
In 4d
hν = 60 eV
Θ
(ML)
1.5
0.7
0.3
0.1
0
Θ
(ML)
35.0
15.0
6.0
2.7
1.5
0
15.0
6.0
2.7
1.5
0
37
38
39
36
37
38
39
40
n(E) (arbitrary units)
kinetic energy (eV)

Figure 1

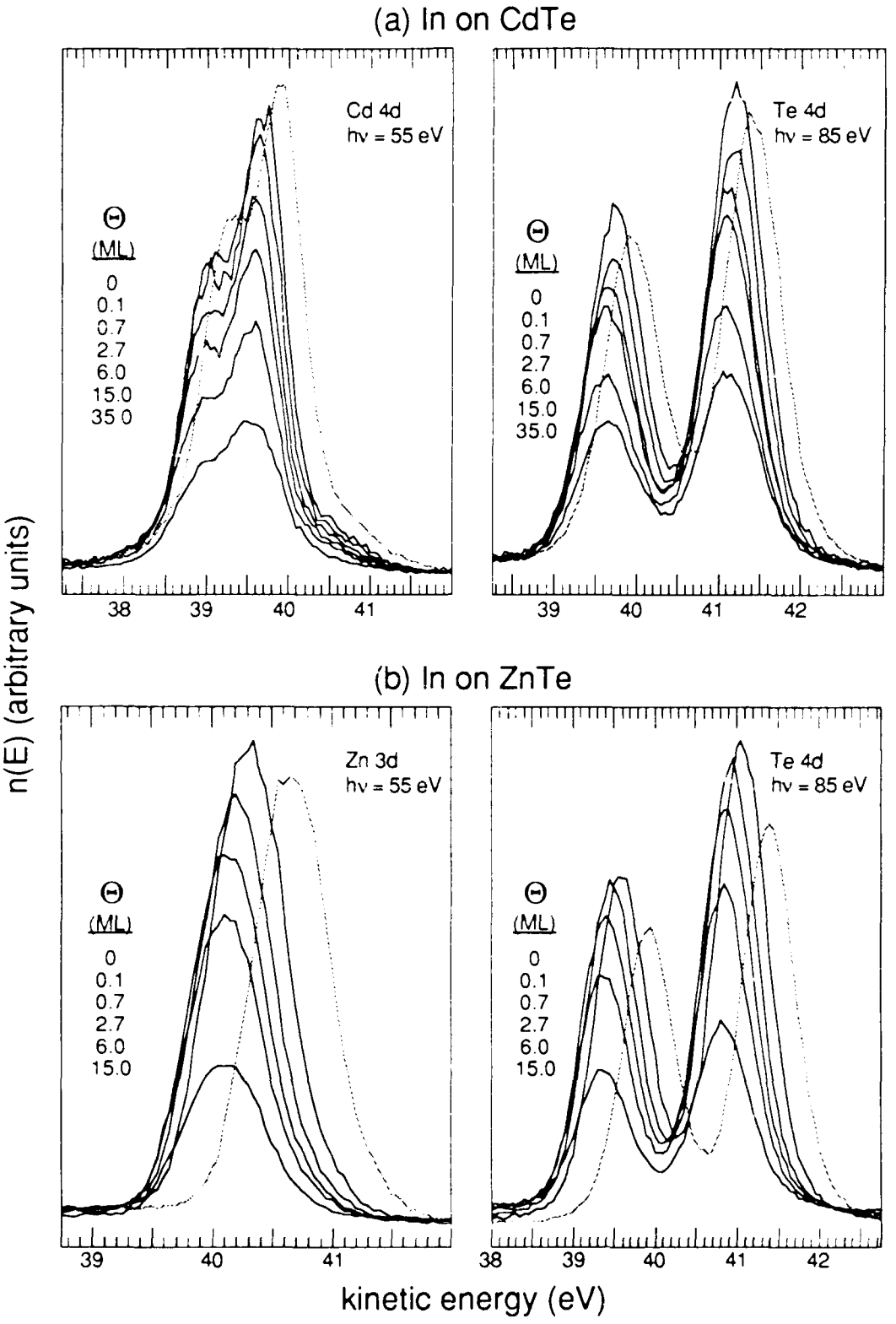
(a) In on CdTe
Cd 4d
hν = 55 eV
Θ
(ML)
0
0.1
0.7
2.7
6.0
15.0
35.0
38
39
40
41
Te 4d
hν = 85 eV
Θ
(ML)
0
0.1
0.7
2.7
6.0
15.0
35.0
39
40
41
42
(b) In on ZnTe
Zn 3d
hν = 55 eV
Θ
(ML)
0
0.1
0.7
2.7
6.0
15.0
39
40
41
Te 4d
hν = 85 eV
Θ
(ML)
0
0.1
0.7
2.7
6.0
15.0
38
39
40
41
42
n(E) (arbitrary units)
kinetic energy (eV)

Figure 2

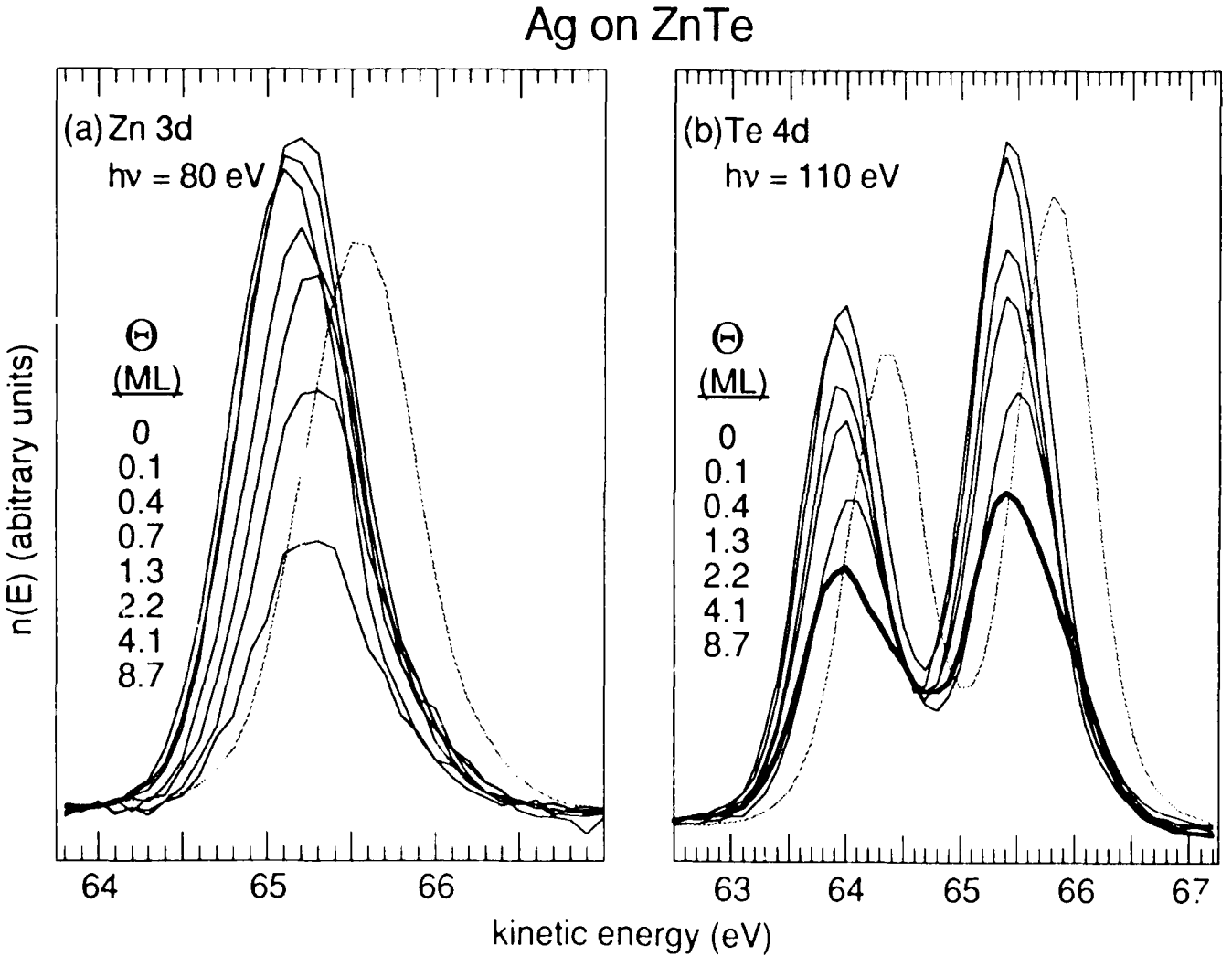
Ag on ZnTe
(a) Zn 3d
hν = 80 eV
Θ
(ML)
0
0.1
0.4
0.7
1.3
2.2
4.1
8.7
(b) Te 4d
hν = 110 eV
Θ
(ML)
0
0.1
0.4
1.3
2.2
4.1
8.7
n(E) (abitrary units)
64
65
66
63
64
65
66
67
kinetic energy (eV)

Figure 3

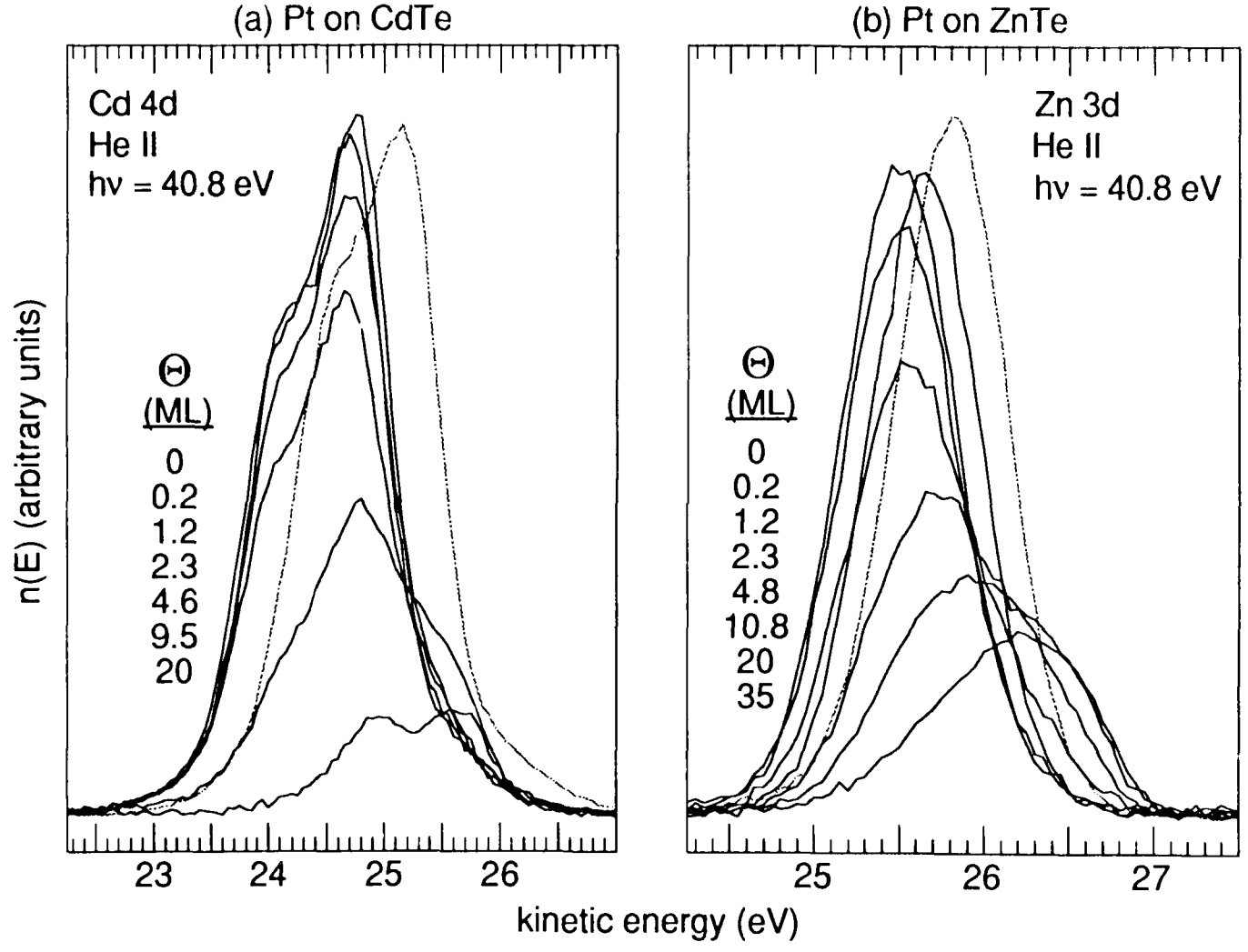
(a) Pt on CdTe
Cd 4d
He II
hν = 40.8 eV
Θ
(ML)
0
0.2
1.2
2.3
4.6
9.5
20
(b) Pt on ZnTe
Zn 3d
He II
hν = 40.8 eV
Θ
(ML)
0
0.2
1.2
2.3
4.8
10.8
20
35
n(E) (arbitrary units)
23
24
25
26
25
26
27
kinetic energy (eV)

Figure 4

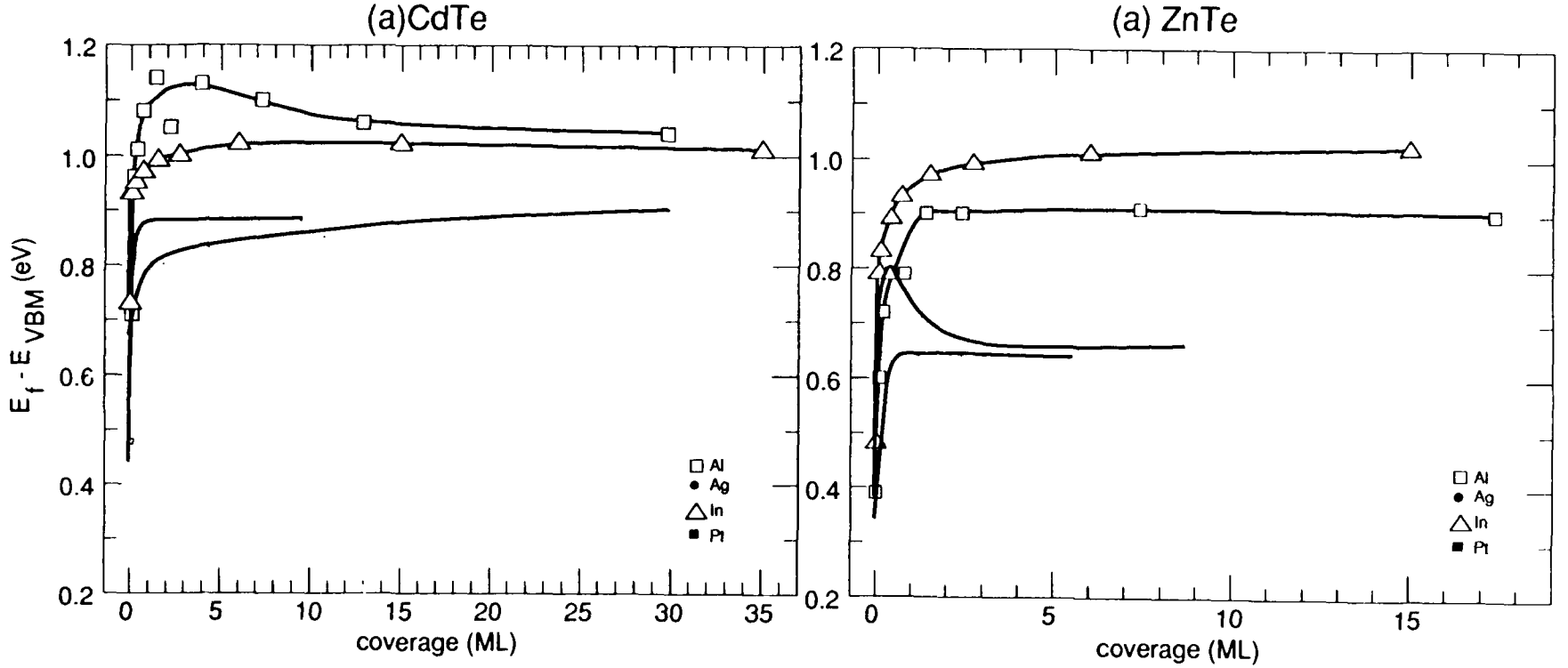
(a)CdTe
(a) ZnTe
$E_f - E_{VBM}$ (eV)
1.2
1.0
0.8
0.6
0.4
0.2
0
5
10
15
20
25
30
35
coverage (ML)
Al
Ag
In
Pt

Figure 5

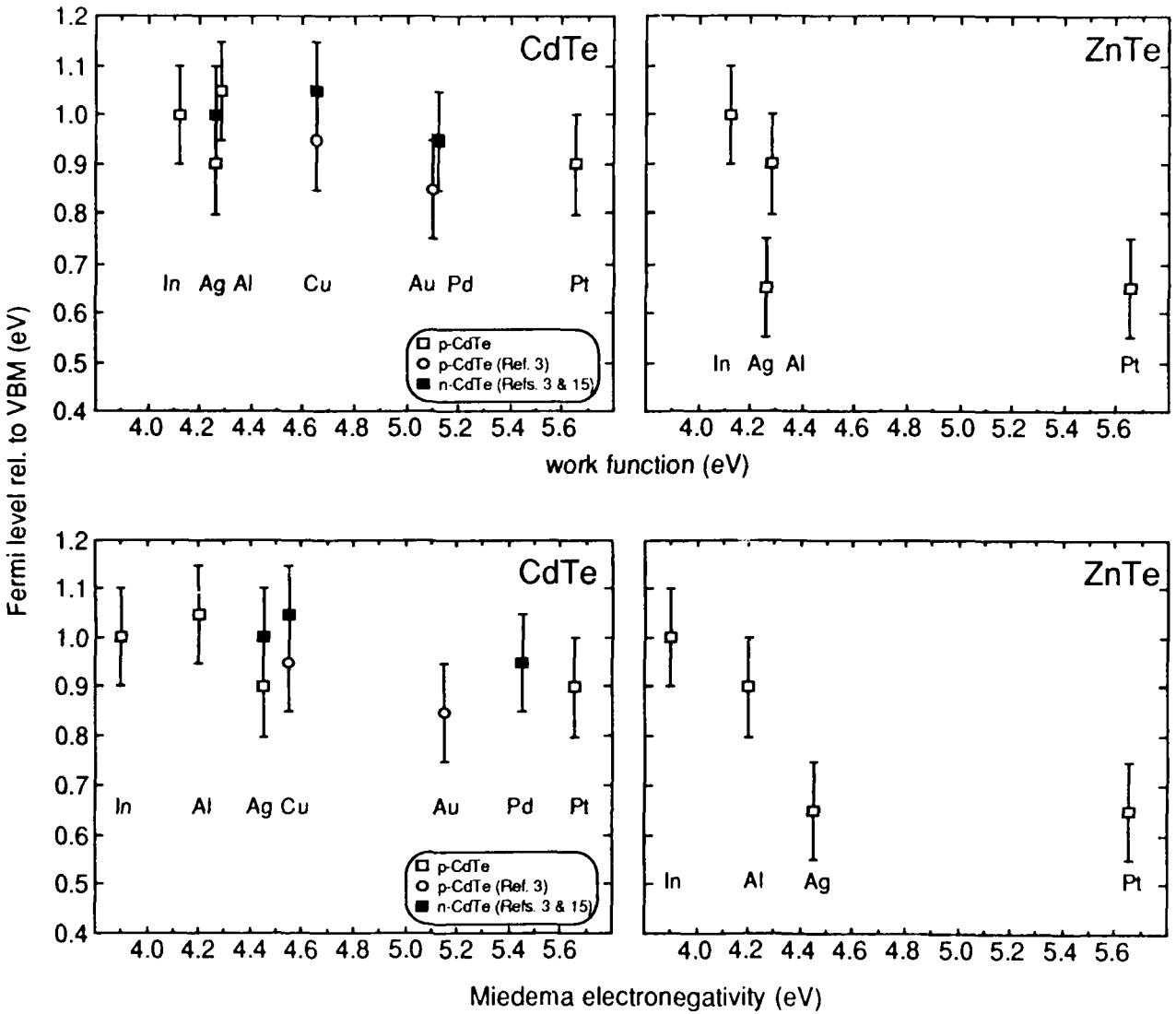
CdTe
ZnTe
In Ag Al Cu Au Pd Pt
In Ag Al Pt
In Al Ag Cu Au Pd Pt
In Al Ag Pt
p-CdTe
p-CdTe (Ref. 3)
n-CdTe (Refs. 3 & 15)
Fermi level rel. to VBM (eV)
work function (eV)
Miedema electronegativity (eV)
1.2
1.1
1.0
0.9
0.8
0.7
0.6
0.5
0.4
4.0 4.2 4.4 4.6 4.8 5.0 5.2 5.4 5.6

Figure 6